

## Analysis of the Henderson–Abraham–Barker equation in the case of a polar liquid near a neutral hard wall

J. P. Badiali, V. Russier, and M. E. Holovko

Citation: *The Journal of Chemical Physics* **99**, 8051 (1993); doi: 10.1063/1.465631

View online: <http://dx.doi.org/10.1063/1.465631>

View Table of Contents: <http://scitation.aip.org/content/aip/journal/jcp/99/10?ver=pdfcov>

Published by the [AIP Publishing](#)

---

### Articles you may be interested in

[Structure of a dipolar hard sphere fluid near a neutral hard wall](#)

J. Chem. Phys. **96**, 4639 (1992); 10.1063/1.462800

[Analysis of the BarkerHenderson localcompressibility approximation. II. Comparison with other theories of liquids](#)

J. Chem. Phys. **58**, 876 (1973); 10.1063/1.1679341

[Saturated Liquid Properties from the Mie\(n, 6\) Potential and the BarkerHenderson Perturbation Theory](#)

J. Chem. Phys. **57**, 4575 (1972); 10.1063/1.1678119

[Analysis of the Barker—Henderson LocalCompressibility Approximation](#)

J. Chem. Phys. **55**, 3794 (1971); 10.1063/1.1676664

[Note on the Perturbation Equation of State of Barker and Henderson](#)

J. Chem. Phys. **51**, 5295 (1969); 10.1063/1.1671948

---



# Analysis of the Henderson–Abraham–Barker equation in the case of a polar liquid near a neutral hard wall

J. P. Badiali and V. Russier

*Structure et Réactivité des Systèmes Interfaciaux, Université Pierre et Marie Curie, URA 1662 du CNRS, Bat. F, 4 Place Jussieu, 75230 Paris Cedex 05, France*

M. E. Holovko

*Theory of Solutions, Institute of Condensed Matter Physics, Ukrainian Academy of Sciences, Svientsitski Street, 290011 Lviv, Ukraine*

(Received 28 June 1993; accepted 2 August 1993)

The physical content of the wall–particle direct correlation function  $c_w(1)$ , defined from the Ornstein–Zernike equation in the framework of the Henderson–Abraham–Barker approach, is analyzed in the case of a dipolar-hard-sphere fluid near a pure and dielectric neutral wall. The exact asymptotic behavior of  $c_w(1)$  is established and we show that it is not related to simple physical concepts as, e.g., the image potential. We show that the exact Henderson–Abraham–Barker equation introduces some bridge diagrams which are more simple graphs in another approach. Due to this fact, at least for systems with long range interactions, it is misleading to use the usual closures of the theory of homogeneous liquids for  $c_w(1)$ . In the case of a dielectric wall, we emphasize that the diagrammatic structure of  $c_w(1)$  requires the introduction of a three-body Mayer function. The dipolar-hard-sphere liquid is a good candidate for analyzing  $c_w(1)$  because some exact results are known and related to simple electrostatic effects; however, the present results are not restricted to this system.

## I. INTRODUCTION

The structure of inhomogeneous dipolar-hard-sphere fluids can be characterized by the probability  $\rho(1)$  of finding the molecule 1 at a given position and with a given orientation. Hereafter “1” will represent both the position and the orientation of the molecule 1. Instead of  $\rho(1)$ , it is convenient to use  $h(1)=[\rho(1)-\rho]/\rho$ , where  $\rho$  is the number density in the bulk phase. One of the most popular theoretical tools introduced for calculating  $h(1)$  is the so-called Henderson–Abraham–Barker (HAB) equation.<sup>1</sup> It results from the Ornstein–Zernike equation, where the wall is considered as a giant hard-sphere particle. We thus introduce a wall–molecule direct correlation function  $c_w(1)$ , and  $h(1)$  is related to the direct correlation function of the bulk fluid  $c(1,2)$  according to

$$h(1)=c_w(1)+\rho\int h(2)c(1,2)d2, \quad (1)$$

where the integration is performed over the position and orientation of 2. We may consider Eq. (1) as a definition of  $c_w(1)$  and, as usual, the closure of the HAB equation requires a second relation between  $c_w(1)$  and  $h(1)$ . Since Eq. (1) is obtained by considering first an homogeneous mixture, it is very tempting to approximate  $c_w(1)$  by using the closure relations (mean-spherical approximation, MSA, Percus–Yevick, PY, or hypernetted chain, HNC) which have proved to be efficient in the case of homogeneous systems. In particular, such an approach has been used extensively for calculating the structure of polar and ionic systems near a planar hard wall.<sup>2</sup>

In a recent paper,<sup>3</sup> it has been shown analytically that the use of the HAB equation with the HNC closure, hereafter noted the HAB-HNC closure, leads to very poor re-

sults when focusing on the asymptotic behavior of  $h(1)$  in the case of a polar liquid near a neutral planar interface. The HAB-HNC closure reproduces the correct result only at the lowest order in density. The asymptotic behavior corresponds to regions far from the wall where  $h(1)$  is extremely small; nevertheless, this region is governed by electrostatics and there we can investigate whether the approximations used reproduce the electrostatic results we must recover in any case. For example, it has been established that the potential of mean force at infinite dilution for an ion in a polar liquid near a planar wall exhibits an asymptotic behavior which results exactly from a pure electrostatic effect. No closure such as the HAB-HNC one, e.g., is able to reproduce this simple result. A numerical test of the HAB-HNC closure has been presented in Ref. 4.

The main goal of this paper is to elucidate the physical content of  $c_w(1)$ . In order to do that, we calculate the exact asymptotic behavior of  $c_w(1)$ , in the case of a dipolar-hard-sphere fluid near a neutral planar wall. The interaction between particles of the fluid is given simply by the sum of the hard sphere potential  $V_{hs}(1,2)$  and the classical dipole–dipole interaction  $V_{dd}(1,2)$ . In Sec. II of this paper, the wall is only an infinite repulsive barrier without any dielectric property, i.e., its dielectric constant  $\epsilon_w$  is unity. In Sec. III, the wall is characterized by a dielectric constant  $\epsilon_w$  different from 1. As we shall see, this requires a nontraditional version of the HAB equation. The so-called self-image potential must appear in the wall–molecule pair potential, but in order to reproduce the image potential between a pair of molecules in the fluid, a three-body potential involving the two molecules and the wall must be introduced. In the last section, we discuss some general aspects of our results and the relation with some approximate closures as the HAB-HNC one.

## II. THE PURE HARD WALL

From the exact relation between the profile  $\rho(1)$  and the one-body direct correlation function  $c(1)$  (see, e.g., Ref. 5), we can write  $\ln[1+h(1)]=c(1)-c(\infty)$ , where  $c(\infty)$  is the value of  $c(1)$  in the bulk phase. When focusing on the asymptotic behavior of the profile, we have simply  $h_{as}(1)=c(1)-c(\infty)$ . In Ref. 6, it has been shown that  $h_{as}(1)$  satisfies the following equations:

$$h_{as}(1)=R(1)+\rho \int R(2)h(1,2)d2 \quad (2)$$

or

$$h_{as}(1)=R(1)+\rho \int h_{as}(2)c(1,2)d2, \quad (3)$$

where  $h(1,2)$  is the total correlation function in bulk phase.  $R(1)$  is a surface quantity representing an infinite sum of ring graphs; it is given by

$$R(1)=-(\beta\mu^2/16)[(\epsilon-1)/\epsilon(\epsilon+1)][(\epsilon-1)/3y]^2 \times (1/z_1^3)\Sigma_l \gamma(2l)Y_{2l}^0(\mu_1), \quad (4)$$

in which  $\beta=1/k_B T$ ,  $\mu$  is the magnitude of the dipole moment,  $\epsilon$  is the dielectric constant of the bulk liquid,  $z_1$  is the distance from the wall,  $y=4\pi\rho\beta\mu^2/9$ ,  $Y_{2l}^0(\mu_1)$  is the usual spherical harmonic characterizing the orientation of the dipole moment and, finally,  $\gamma(2l)$  is a particular integral of an angular component of the triplet direct correlation function in the bulk phase. The sum in Eq. (4) runs over all the positive values of the integer  $l$ . In the system we study here, we emphasize that *a priori* the only quantity presenting a simple meaning is the image potential acting on a dipole, due to its interaction with the images of all the other dipoles of the fluid. Thus we can consider that a given quantity (correlation function,...) has a simple physical meaning if it can be simply related to this image potential. This is the case of the function  $R(1)$ , since as shown in Refs. 6 and 7, its  $l=0$  component,  $R_{l=0}(1)$ , is proportional to  $(-\beta)$  times the angular average of the image potential; the ratio between these two quantities is related to the electrostriction constant and is always positive.

Although Eqs. (1) and (3) have a similar form, the comparison of these two equations requires a careful analysis. First of all, in opposition to Eq. (1) which is exact whatever the value of  $z_1$ , Eq. (3) only gives the asymptotic behavior of  $h(1)$ . Second, Eqs. (1) and (3) are based on different diagrammatic representations. In the derivation of Eq. (1), the wall is first considered as a particle and accordingly  $c_w(1)$  represents the sum of graphs, free of nodal point, connecting the wall particle to the molecule 1; in these graphs, each field point is weighted by the bulk density  $\rho$ . In Eq. (3), the wall is considered from the beginning and each field point " $i$ " is weighted by the actual profile  $\rho(i)$ . At first glance, it seems tempting to identify  $c_w(1)$  and  $R(1)$ ; as we shall see below, this is not exact and therefore  $c_w(1)$  is found to present no simple meaning.

In order to illustrate the difference between the two diagrammatic representations, we consider the density expansion of  $h(1)$ . The results have been already presented

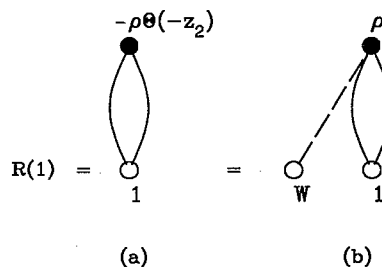


FIG. 1. Diagrammatic expression of  $R(1)$  at the order  $\rho$ . The solid line represents  $[-\beta V_{dd}(1,2)]$ ; the dashed line represents  $-\theta(-z_2)$ . (a) is a part of a ring graph, while (b), which has a nodal point, does not contribute to the wall-particle direct correlation function  $c_w(1)$ .

in Ref. 7 and the details will be not reported here. At the lowest order in density, the one-body direct correlation function  $c(1)$  is simply the integral of the Mayer function  $f(1,2)$  weighted by the profile  $\rho(2)$  which at this order is the step profile. The quantity  $c(\infty)$  has the same definition as  $c(1)$ , but we must use  $\rho$  instead of  $\rho(2)$ . The relation  $h_{as}(1)=c(1)-c(\infty)$  leads to

$$h_{as}(1)=-\rho \int \theta(-z_2)f(1,2)d2 \\ =-\rho \int \theta(-z_2)(1/2)[- \beta V_{dd}(1,2)]^2d2. \quad (5)$$

In the last integral, the Mayer function  $f(1,2)=(\exp[-\beta[V_{hs}(1,2)+V_{dd}(1,2)]]-1)$  has been expanded in terms of  $\beta V_{dd}(1,2)$  in order to get the asymptotic behavior.<sup>7</sup> The function  $h_{as}(1)$  given by Eq. (5) is equal to  $R(1)$  and its diagrammatic expansion is given by Fig. 1(a). Now, in the HAB description, the molecule 2 must be related to the wall and  $\rho$  is the weight associated to 2. Since the wall is like a pure hard sphere, the corresponding Mayer function is  $(-1)$  if  $z_2 < 0$  and zero elsewhere; it coincides therefore with the step function  $\theta(-z_2)$ . Then, in the HAB description, Eq. (5) is represented by Fig. 1(b). Figures 1(a) and 1(b), which have the same value, correspond to very different diagrammatic structures. In Fig. 1(a), we have a ring graph—it is a part of the one-body-direct correlation function and corresponds to  $R(1)$ . In Fig. 1(b), 2 is a nodal point and then Fig. 1(b) cannot be a part of the direct correlation function  $c_w(1)$ . Accordingly, we cannot identify  $c_w(1)$  and  $R(1)$ .

At higher densities, any graph of  $R(1)$  in which, at least, two field points are connected to the wall contributes to  $c_w(1)$ . Thus the difference between  $R(1)$  and  $c_w(1)$  comes from the infinite sum of graphs in which only one field point is connected to the wall. From the results given in Refs. 6 and 7, the diagrammatic picture of  $[c_w(1)-R(1)]$  is shown in Fig. 2.

The same result can be also obtained by considering the HAB equation directly. Let us consider a reference system which is a pure hard sphere fluid near a neutral wall. Then  $h(1)$ ,  $c(1,2)$ , and  $c_w(1)$  become, respectively,

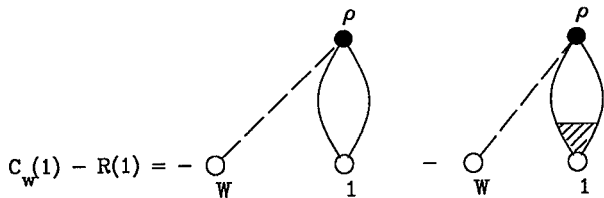


FIG. 2. Diagrammatic representation of  $c_w^{\text{as}}(1) - R(1)$ . The solid line represents  $h^L(1,2)$ , the long range part of the total correlation function  $h(1,2)$  in the bulk phase. In the last graph, the hatched part represents the bulk triplet direct correlation function and the dashed line means  $-\theta(-z_2)$ . This graph is clearly a bridge diagram.

$h^{\text{hs}}(1)$ ,  $c^{\text{hs}}(1,2)$ , and  $c_w^{\text{hs}}(1)$ . We subtract from Eq. (1) the HAB equation corresponding to the reference system and obtain

$$\begin{aligned} \delta h(1) = & \delta c_w(1) + \rho \int \delta h(2) c(1,2) d2 \\ & + \rho \int h^{\text{hs}}(2) c(1,2) d2 \\ & - \rho \int h^{\text{hs}}(2) c^{\text{hs}}(1,2) d2, \end{aligned} \quad (6)$$

where  $\delta h(1) = h(1) - h^{\text{hs}}(1)$  and  $\delta c_w(1) = c_w(1) - c_w^{\text{hs}}(1)$ . When focusing on the asymptotic behavior,  $\delta h(1)$  is identical to  $h_{\text{as}}(1)$  and  $\delta c_w(1)$  is the asymptotic part  $c_w^{\text{as}}(1)$  of  $c_w(1)$ . In Eq. (6), we can drop the last term and we get

$$\begin{aligned} c_w^{\text{as}}(1) - \left[ h_{\text{as}}(1) - \rho \int h_{\text{as}}(2) c(1,2) d2 \right] \\ = -\rho \int h^{\text{hs}}(2) c(1,2) d2. \end{aligned} \quad (7)$$

We can see from Eq. (3) that the bracket is nothing else than  $R(1)$ . Thus, the asymptotic behavior of the difference  $c_w(1) - R(1)$  is determined by the right-hand side of Eq. (7). From the arguments given in Ref. 8, the asymptotic part of the integral comes from the region  $z_2 < 0$ , where  $h^{\text{hs}}(2) = -1$ . This domain selects the long range behavior  $c^L(1,2)$  of the bulk direct correlation function  $c(1,2)$  since  $z_1$  is positive and very large, while  $z_2$  is negative. From the diagrammatic analysis of  $c^L(1,2)$ , we have<sup>6,7</sup>

$$\begin{aligned} c^L(1,2) = & (1/2) [h^L(1,2)]^2 \\ & + (\rho^2/2) \int h^L(1,3) h^L(1,4) c(3,4,2) d3 d4, \end{aligned} \quad (8)$$

in which  $h^L(1,2)$  is the long range part of the bulk total correlation function and  $c(3,4,2)$  is the triplet direct correlation function. After integration over the orientations of 3 and 4, we can see that only the short range part of  $c(3,4,2)$  contributes to the integral. Accordingly, in Eq. (8), we may replace  $h^L(1,3)$  by  $h^L(1,2)$ ,  $h^L(1,4)$  by  $h^L(1,2)$ , and the integration over the positions of 3 and 4 can be performed independently of other positions. Thus,

the bridge diagram represented by this integral can be easily calculated. As expected, Eq. (8) is identical to the result given in Fig. 2.

From the explicit form of  $h^L(1,2)$  given in Ref. 9, we obtain

$$\begin{aligned} c_w^{\text{as}}(1) - R(1) = & (3\beta y \mu^2 / 32 z_1^3) [(\epsilon - 1)/3y]^4 \\ & \times (1/\epsilon^2) \Sigma_l \Gamma(2l) Y_{2l}^0(\mu_1). \end{aligned} \quad (9)$$

From the explicit expression of  $R(1)$  given in Eq. (4), we obtain the following expression for the ratio  $\alpha = c_w^{\text{as}}(1)/R(1)$ :

$$\alpha = c_w^{\text{as}}(1)/R(1) = \{1 - (1/2) [(\epsilon - 1)/3y] [(\epsilon + 1)/\epsilon]\}. \quad (10)$$

The analytical expression of  $\alpha$  represents the main result of this section.

First of all, we study  $\alpha_0$ , the low density value of  $\alpha$ . In order to do that, we use the virial expansion of the dielectric constant<sup>10</sup>  $\epsilon = 1 + 3y + 3y^2(1+b) + O(y^3)$ , where  $b$  is related to the low density limit of the so-called Kirkwood factor  $g$ .<sup>11</sup> At the lowest order in  $y$ , we obtain  $\alpha_0 = y(1/2 - b)$ . Thus,  $c_w^{\text{as}}(1)$  and  $R(1)$  are not of the same order in the density expansion. This is illustrated in Fig. 1—Fig. 1(a) is a part of  $R(1)$ , but Fig. 1(b), in which there is a nodal point, does not contribute to  $c_w^{\text{as}}(1)$ . Thus the leading contribution to  $c_w^{\text{as}}(1)$  must be of the order of  $y^2$ . Moreover the sign of  $\alpha_0$  is not known *a priori*; it depends on the value of  $b$ . The explicit calculation of  $b$ , till the order  $\mu^{*10}$ , where  $\mu^{*2}$  is the reduced dipole moment  $\mu^{*2} = \beta \mu^2 / \sigma^3$ , shows that  $\alpha_0$  will be positive provided  $\mu^* < 1.86$ . Thus, in the low density regime,  $c_w^{\text{as}}(1)$  and  $R(1)$  do not necessarily have the same sign. Now, it is obvious that  $c_w^{\text{as}}(1)$  and  $R(1)$  do not have the same physical content; while  $R(1)$  is related to the image potential, we can conclude that  $c_w^{\text{as}}(1)$  has a more complicated meaning. Clearly this result is not restricted to the low density behavior.

By using the Kirkwood formula<sup>11</sup> which relates the dielectric constant to the Kirkwood factor  $g$ , we obtain

$$\alpha = [1 - (3/2)(\epsilon + 1)g/(2\epsilon + 1)]. \quad (11)$$

For large values of  $\epsilon$ , we have  $\alpha = 1 - 3g/4$ , and the sign of  $\alpha$  is negative if  $g > 4/3$ , a condition which is likely to be fulfilled, since it corresponds (for large  $\epsilon$ ) to  $\epsilon > 6y$  which, to the best of our knowledge, is likely to hold when  $\epsilon$  is large compared to 1. So, also in this case, we see that it is difficult to deduce  $c_w^{\text{as}}(1)$ , even approximately, from simple physical considerations. In the next section, this analysis will be extended to the case of wall having a dielectric constant  $\epsilon_w$  different from unity.

### III. THE CASE OF A DIELECTRIC WALL

In the HAB description, we must introduce explicitly the so-called self-image potential  $U^{\text{SI}}(1)$  defined by

$$U^{\text{SI}}(1) = (\mu^2/16) [(1 - \epsilon_w)/(1 + \epsilon_w)] [(1 + \cos^2 \theta_1)/z_1^3] \quad (12)$$

in the wall-molecule Mayer function  $f_w(1)$  which becomes

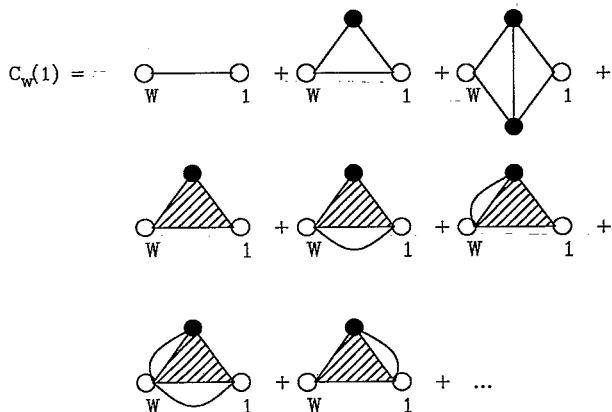


FIG. 3. Diagrammatic expansion of  $c_w(1)$  in the case of a dielectric wall. Here the solid line represents either  $f_w(i)$  or  $f(i,j)$ . The first line of the figure only contains the two-body Mayer function. The second line contains the three-body Mayer function  $f(1,2,w)$ .

$$f_w(1) = \{\exp[-\beta U^{SI}(1)] - 1\}, \quad \text{if } z_1 > 0$$

and

$$f_w(1) = -1, \quad \text{if } z_1 < 0. \quad (13)$$

In Eq. (12),  $\theta_1$  is the polar angle of the dipole moment relative to the normal to the surface. Between particles 1 and 2 of the liquid, we have the Mayer function  $f(1,2)$  defined above, but, in addition, we must also introduce a three-body Mayer function  $f(1,2,w)$  including simultaneously the molecules 1 and 2 and the wall  $w$ . The function  $f(1,2,w)$  represents the change in the interaction between 1 and 2 due to the presence of the wall. We have

$$f(1,2,w) = \exp\{-\beta[(1-\epsilon_w)/(1+\epsilon_w)][(\mu_1 \cdot \nabla_1)(\mu_2 \cdot \nabla_2) \times (1/r_{12}^*)]\} - 1, \quad z_1, z_2 > 0, \quad (14)$$

where  $\nabla_i$  means the gradient acting on the position of the molecule " $i$ " and  $r_{12}^* = (r_{12}^2 + 4z_1 z_2)^{1/2}$  is obtained by mirroring one of the positions relative to the plane  $z=0$ .

The HAB equation is still given by Eq. (1),  $c(1,2)$  remains the bulk direct correlation function, and  $c_w(1)$  is the sum of diagrams, free of nodal points, connecting the wall and the particle 1. However, the diagrammatic expansion of  $c_w(1)$  must include  $f(1,2,w)$ .

As an illustration, the first graphs relative to the density expansion of  $c_w(1)$  are drawn in Fig. 3. The first line contains the two-body Mayer functions  $f_w(1)$  and  $f(1,2)$ . At infinite dilution, only  $f_w(1)$ , which is density independent, contributes to the asymptotic behavior  $c_w^{as}(1)$  of  $c_w(1)$ . The second graph contains  $f_w(1)$ , which decreases as  $1/z_1^3$ , but at least one of the other bonds  $f_w(2)$  or  $f(1,2)$  must introduce an electrostatic effect leading to an extra  $1/z_1^3$  contribution. Consequently, this graph, which is of the order  $\rho$ , does not contribute to  $c_w^{as}(1)$ . The second line in Fig. 3 is associated with  $f(1,2,w)$  which is represented by a hatched triangle. It is of order  $\rho$  since 2 is a black circle. At the same order in density, this graph can be decorated by one or two  $f_w(i)$  bonds as indicated in Fig. 3. The sum of these graphs leads to the same structure as

$f(1,2,w)$ , but points 1 and 2 are on the  $z > 0$  side of the interface and this leads to associate a weight  $\rho\theta(z_2)$  to point 2. The last graph which is also of order  $\rho$  is simply  $f(1,2,w)$   $f(1,2)$  and, when decorated by  $f_w(i)$  as previously, the integration over 2 is weighted by  $\rho\theta(z_2)$ . The integration can be performed immediately by using the product rules given in Ref. 6. For example, the part of  $c_w^{as}(1)$  independent of the dipolar orientation is given by

$$c_w^{as}(1) = -\beta(\mu^2/12)[(1-\epsilon_w)/(1+\epsilon_w)](1/z_1^3) + \beta(\mu^2/24)[(1-\epsilon_w)(3+\epsilon_w)/(1+\epsilon_w)^2] \times (3y/z_1^3). \quad (15)$$

$f_w(1)$  gives rise to the first term which is simply  $(-\beta)$  times the self-image potential, as expected. The second term, due to the existence of  $f(1,2,w)$ , is not related to the image potential. Thus, in the case of the dielectric wall,  $c_w(1)$  also appears as a very complicated quantity. Now, we can show that it is true in very general conditions.

Figure 2 still exhibits the difference between  $c_w(1)$  and  $R(1)$ , but now  $R(1)$  is given by [see Eq. (51) of Ref. 6]

$$R(1) = -(\beta\mu^2/16)[(\epsilon-\epsilon_w)/\epsilon(\epsilon+\epsilon_w)][(\epsilon-1)/3y]^2 \times (1/z_1^3)\Sigma\gamma(2l)Y_{2l}^0(\mu_1) \quad (16)$$

and  $c_w^{as}(1)$  is

$$c_w^{as}(1) = -\beta(\mu^2/16)(1/z_1^3)[(\epsilon-\epsilon_w)/\epsilon(\epsilon+\epsilon_w)] - [(\epsilon-1)/3y]^2(1/2\epsilon)\Sigma\gamma(2l)Y_{2l}^0(\mu_1). \quad (17)$$

If the two dielectric constants  $\epsilon$  and  $\epsilon_w$  are equal, Eq. (17) leads to

$$c_w^{as}(1) = +\beta(\mu^2/16)(1/z_1^3)[(\epsilon-1)/3y]^2 \times (1/2\epsilon)\Sigma\gamma(2l)Y_{2l}^0(\mu_1), \quad (18)$$

while  $R(1)=0$ . This is a very clear demonstration that  $c_w^{as}(1)$  is not related to the image potential. Now, we consider the case where  $\epsilon$  and  $\epsilon_w$  are different; as before, we introduce the ratio  $\alpha = c_w^{as}(1)/R(1)$  which is given by

$$\alpha = [1 - (1/2)(\epsilon-1)^2(\epsilon+\epsilon_w)/3y\epsilon(\epsilon-\epsilon_w)]. \quad (19)$$

If  $\epsilon$  is smaller than  $\epsilon_w$ , then  $\alpha$  is greater than 1. In particular, this will be true if the wall is a perfect metal, since in this case, we have  $\epsilon_w = \infty$  and  $\alpha = [1 + (1/2)(\epsilon-1)^2/3y\epsilon]$ . As expected, when  $\epsilon_w = 1$ , we recover the result obtained in Sec. II. In any case, we see that the magnitude of  $\alpha$  depends on  $\epsilon$ ,  $\epsilon_w$ , and  $y$ .

It is interesting to follow the value of  $\alpha$  [and of  $c_w^{as}(1)$ ] with the increasing of the density at a given value of  $\epsilon_w$ . When the density is small enough, the dielectric constant in the liquid side of the interface is smaller than  $\epsilon_w$  and we get the following scheme: At infinite dilution,  $c_w^{as}(1)$  and  $R(1)$  are now identical in being opposite to the result given by Eq. (11). Moreover  $c_w^{as}(1)$  is just  $[-\beta U^{SI}(1)]$ , which corresponds to the intuitive expectation. At order  $\rho$ ,  $c_w^{as}(1)$  includes  $[-\beta U^{SI}(1)]$  plus an additional term represented by the sum of the diagrams of Fig. 4, including one black point and one  $f(1,2,w)$  bond;

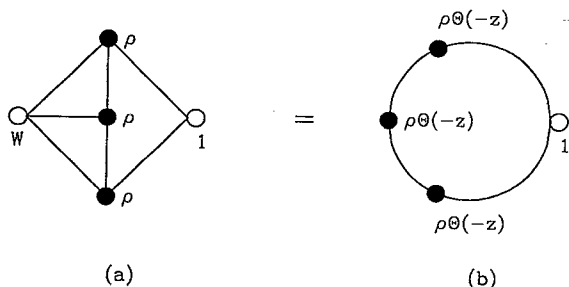


FIG. 4. Example of different diagrammatic representations of same function. (a) corresponds to a bridge diagram of the HAB equation; (b) corresponds to a ring graph involved in the calculation of  $c(1)$ .

this term corresponds to the low density limit of the “other image” contribution discussed in Ref. 12. This is simply the interaction of the images of all the dipoles, with the dipole fixed in 1. Therefore, at this order,  $c_w^{as}(1)$  still results from a simple physical picture and furthermore at order  $\rho$ , and for  $\epsilon_w > \epsilon$ ,  $\alpha$  is given by  $\alpha = [1 + (3\gamma/2)(1 + \epsilon_w)/(\epsilon_w - 1)]$ , which is greater than 1 and thus positive. However, at higher orders in density, this simple physical picture disappears and with the increasing in density when  $\epsilon$  becomes higher than  $\epsilon_w$ , the sign of  $\alpha$  may change if  $(\epsilon - \epsilon_w)/(\epsilon + \epsilon_w) < (1/2)(\epsilon - 1)^2/3\gamma\epsilon$ .

These results prove clearly that  $c_w(1)$  and  $R(1)$  do not have the same physical content and  $c_w(1)$  is not a simple quantity that we may approximate by using a physical intuition as has been proposed in Ref. 12.

#### IV. DISCUSSION

In the HAB formalism, the basic problem is to determine the so-called wall-particle direct correlation function  $c_w(1)$ . We show in this paper that the price we have to pay for the apparent simplicity of the HAB equation is the introduction of  $c_w(1)$ , which has a very intricate physical content. For example, we have shown that  $c_w(1)$  is related to a simple quantity such as the image potential only when  $\epsilon_w \neq 1$  and at first order in density. Although  $c_w(1)$  and the image potential vary as  $1/z_1^3$  when  $z_1$  is large enough, these two quantities may have an opposite sign. The complicated nature of  $c_w(1)$  results from its particular diagrammatic definition in which the wall is considered as a giant particle. In the HAB equation, the graphs in which there is a nodal point between  $w$  and 1 are eliminated from  $c_w(1)$ . However, if we start from the description of the inhomogeneous system via the one-body direct correlation function  $c(1)$ , the wall is just an external field and the

graphs eliminated in  $c_w(1)$  are some of the ring graphs contributing to  $c(1)$  and giving a simple physical meaning to  $R(1)$ . The HAB equation and the calculation of the profile from  $c(1)$  represent two exact starting points for describing inhomogeneous systems. However, in these two approaches, we are dealing with very different diagrammatic expansions. This is illustrated clearly in Fig. 1. The existence of different diagrammatic representations may lead to different assumptions for the closure. In Fig. 4 the graph (a) is a bridge diagram in the HAB approach, but the same graph can be also considered as a ring graph [Fig. 4(b)] contributing to  $c(1)$ . In the HAB-HNC closure, the graph of Fig. 4(a) is neglected, as we neglect the bridge diagrams in the study of homogeneous systems, but the use of a same closure for bulk and inhomogeneous systems is not justified when we start from the HAB equation. First of all, in this case, the wall is a “giant particle” having an infinite diameter; this “particle” offers a very large space in which a large number of particles of the liquid phase can take place. Due to this difference in size, it is not justified to drop the bridge diagrams. Indeed, the infinite sum of these bridge diagrams can be calculated analytically, at least for finding the asymptotic behavior. All these graphs bring the same contribution to the final result.

In the case of a dielectric wall, the diagrammatic definition of  $c_w(1)$  requires the introduction of a nontrivial three-body Mayer function, no similar thing appears if we start from  $c(1)$ .

In this paper, the dipolar-hard-sphere fluid appears to be a good candidate for analyzing the physical content of the HAB equation since, in this case, some exact results can be obtained. In addition, some of them can be predicted, at least partially, from simple electrostatic considerations. However, it is very clear that the main points of this analysis remains true whatever the system under consideration, provided that the interparticle interaction includes a long ranged part.

<sup>1</sup>D. Henderson, F. F. Abraham, and J. A. Barker, *Mol. Phys.* **31**, 1291 (1976).

<sup>2</sup>L. Blum, *Adv. Chem. Phys.* **78**, 171 (1990).

<sup>3</sup>D. R. Berard and G. N. Patey, *J. Chem. Phys.* **95**, 5281 (1991).

<sup>4</sup>Q. Zhang, J. P. Badiali, and M. L. Rosinberg, *J. Mol. Liquids* **48**, 129 (1991).

<sup>5</sup>J. P. Hansen and I. R. McDonald, *Theory of Simple Liquids* (Academic, London, 1986).

<sup>6</sup>Q. Zhang, J. P. Badiali, and W. H. Su, *J. Chem. Phys.* **92**, 4609 (1990).

<sup>7</sup>J. P. Badiali, *J. Chem. Phys.* **90**, 4401 (1989).

<sup>8</sup>J. P. Badiali, *J. Chem. Phys.* **89**, 2397 (1988).

<sup>9</sup>J. S. Hoye and G. Stell, *J. Chem. Phys.* **61**, 562 (1974).

<sup>10</sup>C. G. Joslin, *Mol. Phys.* **42**, 1507 (1981).

<sup>11</sup>J. M. Deutch, *Annu. Rev. Phys. Chem.* **24**, 301 (1973).

<sup>12</sup>D. R. Berard and G. N. Patey, *J. Chem. Phys.* **97**, 4372 (1992).